Exploring extra dimensions with updated constraints on the variation of the Newton's Constant

Gabriele Montefalcone
Advisor: Professor Paul Steinhardt

May 7, 2020

This paper represents my own work in accordance with University regulations.
/s/Gabriele Montefalcone

Abstract

It was recently published a study based on the Swampland picture of string theory, where the authors P. Agrawal, G. Obied, P. J. Steinhardt and C. Vafa investigated the implications of two postulated Swampland criteria for periods of cosmic acceleration showing a strong tension when considering models with a cosmological constant and imposing tight constraints on the possible quintessence models. [1] These results were comparable to a study carried out almost 10 years ago by D. Wesley and P. Steinhardt, whose approach was completely different and based on a set of assumptions that apply to a wide range of compactified models. Specifically, they considered models that are described by: Einstein's theory of general relativity both in the 4d and higher dimensional theory up to small corrections; a conformally flat or simply flat Ricci metric; a spatially flat 4d-theory with bounded extra-dimensions. The key observation of their work is that the accelerated expansion of the large three spatial dimensions causes the compactified extra-dimensions to vary with time and thus impact the value of w_{DE} and $\dot{G}$ in the 4d effective theory, in such a way to make them inconsistent with observations. [2]

In this paper, I will use the same methodology described in [3] to investigate different NEC/CRF models based on the updated constraint on $\left.\frac{\dot{G}}{G}\right|_{\text{today}}$ and using the upper bound on the time-changing w_{DE} as predicted in [1]. Based on the assumptions described above, the results seem to suggest the impossibility to construct models for theories of extra dimensions that satisfy both the instantaneous and secular constraints on the variation of G without having to introduce rather "exotic" terms.

For a compact introduction to General Relativity and some useful relations that I will use throughout the paper to study the different NEC/CRF models, please refer to app.A.

1 Introduction

Periods of cosmic acceleration play a crucial role in a number of cosmological models. Current data show that the universe is now undergoing a period of acceleration. The source for this recent cosmic acceleration takes the name of "dark energy".

Despite the strong research efforts made in the last decades, the nature and properties of dark energy are still unknown and constitute one of the biggest mysteries in modern physics. In sec.1.1 and 1.2, I describe respectively the evidence accumulated and the possible candidates for this mysterious component that is causing the universe to accelerate.

1.1 The Universe is accelerating: evidence for Dark Energy

Since the first "discovery" of this acceleration in the 1990s, mounting evidence has been accumulated. In particular, three important pieces of evidence come from distance measurements of Type Ia supernovae (SNe Ia), the cosmic microwave background (CMB) and studies of the constraints given by the combination of independent measurements on different cosmological models. [1]

Distance measurements of Type Ia supernovae: The first piece of evidence refers to the results published independently in 1998 by two research groups (the High-redshift Supernova Sear [4] and the Supernova Cosmology Project [5]) which studied the relationship between distance and red-shifts of multiple Type Ia supernovae and came to the same conclusion that the universe has to be currently experiencing a period of cosmic acceleration.
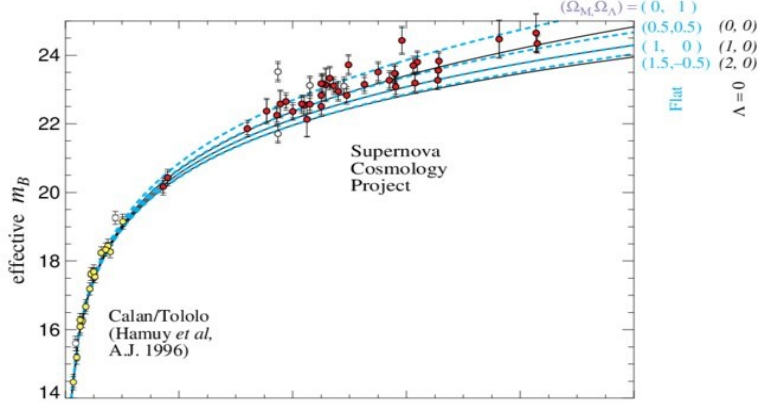
The relationship between distance and red-shifts of galaxies was at first used by Hubble in 1929 and provided compelling evidence for an expanding universe. In this picture, the red-shift of electromagnetic waves is simply caused by their travelling through an expanding space which stretches out their wavelength. The simplest way to measure if this expansion is accelerating or not is therefore to enlarge this research to higher red-shifts and more distant objects in order to obtain a correlation of distance to red-shifts over time.[2]

For this purpose it becomes crucial to measure objects whose absolute luminosity is well known such that one can measure their relative distance by comparing their observed brightness with their known luminosity. These classes of objects are called standard candles. The spectral properties, absolute magnitudes, and light curve shapes of the majority of Type Ia Supernova

---

[1]In all of these researches, dark energy was assumed to be the cosmological constant Λ. Indeed, Λ constitutes a gravitationally self-repulsive form of vacuum energy, initially introduced by Einstein in order to obtain a static model of the universe and balance the attractive action of gravity. This gravitational self-repulsiveness is also a necessary condition for any dark energy candidate in order to ensure the expansion of the universe to accelerate. Therefore, it is important to emphasize that when the researches I cited refer to Λ, they are referring to it as a possible explanation for the current cosmic acceleration.

[2]In this context, it is important to emphasize the intrinsic relationship between space and time. Since light travels at a constant speed c, the light observed from more distant objects was emitted earlier in time and therefore it provides information about the state of the object in the past, at the time of emission.
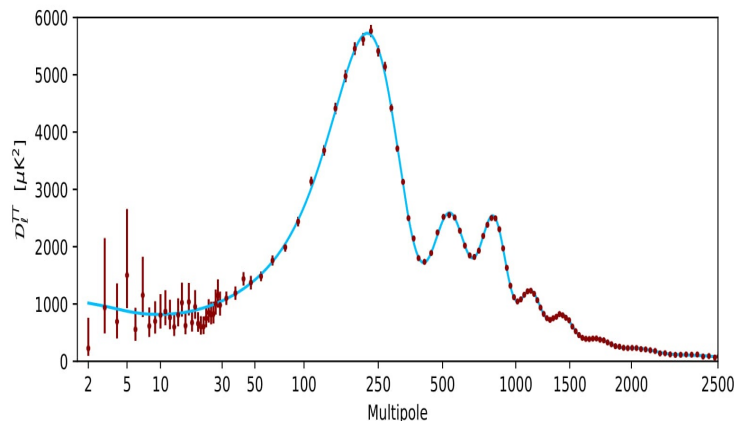
Figure 1: Top panel: Hubble diagram for 42 high-redshift type-Ia supernovae from the Supernova Cosmology Project, and 18 low-redshift ones from the CalÃ¡n/Tololo Supernova Survey. The theoretical predictions for models with different values of Ω_m, Ω_Λ are also shown. Central panel: magnitude residuals from the best-fit flat cosmology ($\Omega_m = 0.28$, $\Omega_\Lambda = 0.72$); the inconsistency between the data and a flat model without a cosmological constant is evident. Bottom panel: uncertainty-normalized residuals from the best-fit flat cosmology Credit: [5]

(SN Ia) are remarkably homogeneous, exhibiting only subtle spectroscopic and photometric differences. [6] SN Ia are also incredibly bright, allowing to be detected even at large distances beyond the local group of galaxies. [4] All these properties combined make Type Ia Supernova a great candidate as standard candles for studies at large red-shifts.

Fig.1 shows the Hubble diagram for the 42 high-redshift type Ia supernovae from the Supernova Cosmology Project and 18 low-redshift type Ia supernovae from the Supernova Survey, plotted on a linear redshift scale to display details at high redshift. The lower rate of increase of relative distances at higher redshifts is evident. This implies that the rate of the expansion must have been smaller in the past compared to the present and that therefore we are now undergoing a period of cosmic acceleration. Based on these data, Perlmutter *et al.* were indeed able to conclude that $\Omega_\Lambda > 0$ with a 99% confidence level and that, assuming a flat universe, the density of non relativistic matter was constrained to $\Omega_m = 0.28^{+0.09}_{-0.08}$. [5]

The Cosmic Microwave Background The CMB represents the thermal radiation leftover from the separation of matter and radiation following the Big Bang. Before that moment, the universe was filled with a hot plasma of charged particles and photons in thermal equilibrium. As the universe expanded, the temperature and energies of the particles decreased and when the energy density of the plasma dropped under the hydrogen ionization energy, protons and electrons combined to form neutral hydrogen atoms. This led to the decoupling of photons from matter, which were finally free to propagate instead of being constantly scattered by electrons and protons in plasma. These relic photons form the CMB as it is observed today. Indeed, the wavelength of these photons increased over time, due to the expansion of the universe, into the

Figure 2: Planck 2018 temperature power spectrum. A characteristic feature of this spectrum is the position of the first acoustic peak at $l_0 = 220.6 \pm 0.6$ which corresponds exactly to a spatially flat universe. Credit: [8]

microwave region with an average temperature equivalent to $\sim 2.7K$. The temperature map of the CMB (fig. 2) as determined by the Planck mission is very uniform and presents small spatial temperature anisotropies, whose relative amplitude is in the range of 1 part in 10^5. [7]

The study of the distribution and intensity of such anisotropies provides tight constraints on the cosmological parameters and is mainly carried out by the studying of the CMB power spectrum, a plot of the fluctuations in the CMB temperature spectrum at different angular scales.

The shape of the power spectrum (fig.2) is determined by the oscillations in the hot gas of the early universe, instead the information about the composition of the universe and therefore about all the density parameters is locked by the angular peaks of these oscillations. For instance, the position of the first peak gives us the value of the curvature of the universe, while the ratio of heights between the first and second peaks tells us how much of the matter is baryonic. [9]

The most recent analysis was released by the Planck collaboration in 2018 [8] and based on the assumption of a ΛCDM cosmology[3], inferred $\Omega_m = 0.321 \pm 0.013$, $\Omega_\Lambda = 0.6847 \pm 0.0073$ and $\Omega_k = 0.0007 \pm 0.0019$[4]. These results fit well with the cosmological model of a spatially flat universe undergoing positive acceleration.
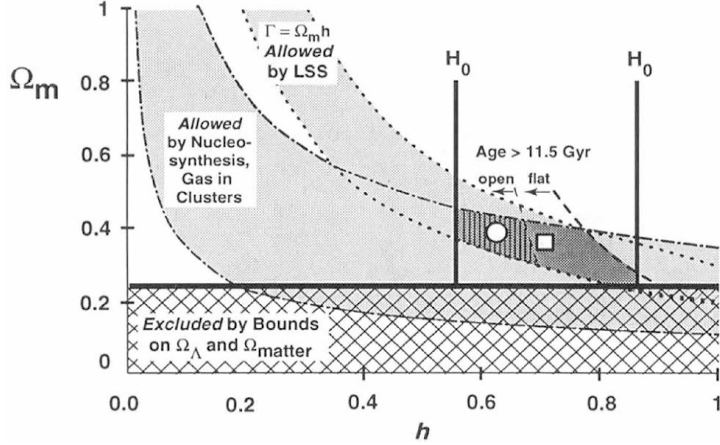
The Cosmic Concordance: Lastly it is worth to briefly discuss the research paper resulted from the joint efforts of J. P. Ostriker and P.J. Steinhardt published in 1995. [10] This work was the first in chronological order to show the consistency of a cosmological model characterized by an accelerating universe.

---

[3]the "standard model" of Big Bang cosmology which assumes three majors components of the universe: matter (byronic and cold dark matter); radiation and the cosmological constant Λ. Please refer to sec.1.2 for a precise description of Λ and its correlation to an accelerating universe.

[4]Recall that Ω_k represents the density parameter of the spatial curvature of the universe, if $\Omega_k > 0$ the universe is closed, if $\Omega_k < 0$ is open and finally, such as in our case, if $\Omega_k = 0$ the universe is flat.

Their approach was completely different from the ones described above. Indeed, they did not make a prediction based upon the single measurement of an experiment, instead, they took the best known astronomical constraints on several cosmological parameters (the matter density Ω_m, the Hubble parameter H_0 and the age of the universe t_0) and combined them to map out a range of models consistent to all of them.

Figure 3: The range of models in concordance with the best known astronomical observations. The entire darkly shaded region (with and without vertical stripes) is the concordance domain for flat models with $\Omega_\mathrm{m} + \Omega_\Lambda = 1$; the vertically striped subregion alone applies to open models with $\Omega_\Lambda = 0$. The square indicates a central, representative flat model with $h = 0.7$, $\Omega_\mathrm{m} = 0.35$ and $\Omega_\Lambda = 0.65$. Credit: [10]

The plot in fig.3 is a map of all the permitted parameter space in the (Ω_m, h) plane[5]. The evidence provided constrains the value of Ω_m to $(0.21 \pm 0.12)h^{-1}$ and it mainly comes from X-ray measurements of gas masses combined with estimates of their total viral mass [11] and light element nucleosynteshis. In regard to the Hubble parameter, the evidence comes from direct observations with the Hubble Space Telescope ($H_0 = 82 \pm 17\,\mathrm{km\,s^{-1}Mpc^{-1}}$) [12] and studies using Type I supernovae ($H_0 = 67 \pm 7\,\mathrm{km\,s^{-1}Mpc^{-1}}$) [13].

Two lower bounds on the age of the Universe (given in billion years) are also considered and are based on re-evaluations of the ages of the oldest clusters using two different methods: the main-sequence turn off ($t_0 = 15.8 \pm 2.1$) [14] and the giant-branch fitting ($t_0 = 13.5 \pm 2.0$) [15]. Finally, the density of the cosmological constant Ω_Λ is considered to be < 0.75, this constraint comes from various tests as described in [16] and most directly by gravitational lensing measurements on quasars.

The range of concordance with all the mentioned observations is represented by the darkly shaded region. This entire section is consistent with flat models with $\Omega_\Lambda > 0$, meanwhile the smaller sub region underlined with vertical stripes is consistent with open models with $\Omega_\Lambda > 0$. The most interesting aspect of this map is the square inside the concordance region which indicates a central, representative flat model with $\Omega_\mathrm{m} = 0.35$ and $\Omega_\Lambda = 0.65$. [10]

---

[5]It is important to emphasize that h is simply defined as the dimensionless Hubble parameter such that $H_0 = h \times 100\,\mathrm{km\,s^{-1}Mpc^{-1}}$

This research was the first one to suggest the strong possibility of a flat universe dominated by the cosmological constant and therefore positively accelerating[6], consistent with all the observations. Their method of combining different independent measurements to obtain constraints on certain parameters now constitutes an essential feature for any cosmological search.

1.2 Dark Energy Candidates

The main implication from our discussion above is that the universe is dominated by some form of dark energy gravitationally self-repulsive which is causing the expansion universe to accelerate. The main distinctive feature of dark energy is that its characteristic pressure p_{DE} needs to be less than $-\frac{1}{3}\rho_{\mathrm{DE}}$ such that $w_{\mathrm{DE}} < -\frac{1}{3}$ and acceleration is ensured.[7]. The are therefore simply two logical candidates for dark energy: a constant and homogeneous vacuum energy equivalent to the cosmological constant Λ and a time-evolving, spatially inhomogeneous component of which many examples can be constructed and that all go under the name of quintessence (Q).

The Cosmological Constant Λ was a term with negative pressure at first introduced by Einstein in its field equations with a value precisely fine-tuned to counteract and balance the attractive action of gravity and ensure a static model of the universe. Today, with Λ, one simply refers to the energy of empty space whose self-repulsive action is causing the universe to accelerate. Its main feature is that is characterized by $w_{\Lambda} = -1$ and is thus uniquely defined by its magnitude Λ . [17] Finally Λ differs from Einstein's original concept in the sense that it is not precisely fine-tuned to balance the gravitational attractive action but it must be overabundant to cause the expansion of the universe to accelerate. [17]

Quintessence Q represents the second logical class of candidate which is a dynamical, evolving and spatially inhomogeneous component with negative pressure. [18] Most models predict an equation of state $-1 < w \leq 0$ since this range fits current cosmological observations best, in comparison to Λ which has exactly $w = -1$. Generally the smaller the value of w the larger its effect on the acceleration of the universe. It is important to notice that in the case of Q the energy density and pressure might evolve in time and consequently be inhomogeneous in space such that the resulting w may not be constant as well. [17] A common model of quintessence is the energy density associated with a scalar field Φ slowly rolling down a potential $V(\Phi)$. Assuming that the scalar field couples with other matter only gravitationally, one can derive the energy momentum tensor $T_{\mu\nu}$ as given in eq.28, from which it follows that $w(\Phi)$ is equal to:

$$w(\Phi) = \frac{p}{\rho} = \frac{\frac{1}{2}\dot{\Phi}^2 - V(\Phi)}{\frac{1}{2}\dot{\Phi}^2 + V(\Phi)} \tag{1}$$

---

[6]It can be shown by solving the Friedman equations that if one considers a flat universe ($\Omega_{\mathrm{k}} = 0$) with $\Omega_{\Lambda} > \Omega_{\mathrm{i}}$ for all the other i components, $\ddot{a} > 0$.

[7]as shown in Appendix .A the condition for an accelerating universe is $w < -\frac{1}{3}$

The motivation for considering a quintessential model for dark energy relates to its dynamic nature which allows for a lot of potentially interesting implications which could be experimentally checked and gives us some insight about fundamental physics and the overall history of the universe. [18]

2 Implications of $\ddot{a} > 0$ in String Theory

In section 1.1 I have presented compelling evidence that shows that the present universe is dominated by some form of dark energy which is causing the universe to accelerate its expansion. Given the mounting evidence for the current cosmic acceleration, when considering any proposed theory of the universe, it becomes crucial to investigate what are the implications and criteria that such theory needs to satisfy in order to allow for an accelerating universe in the present day without violating any of the fundamental assumptions from which the theory itself was derived.

2.1 String theory: Vacuum states, the String Landscape and the Swampland

String theory can be considered as the most structured attempt of a theory of "everything". String theory was at first introduced in the attempt to develop a theory of quantum gravity and it constitutes a theoretical framework where point-like particles are replaced by vibrating strings, in order to eliminate the singularity problem. [19] There are many forms of String theory, all of which require the introduction of extra-dimensions in order to be mathematically consistent.

An important consequence of String theory is the so called "Landscape" which refers to the vast collection of all possible choices for the parameters of compactified models consistent with a quantum theory of gravity. [20] The Landscape is also referred as the collection of all possible vacua. A vacuum state in quantum field theory is defined as the state with the lowest possible energy. A true vacuum is a global minimum of the energy, and is therefore stable. On the other hand, a false vacuum corresponds to a local minimum of the energy and is therefore not stable since, according to the rules of quantum mechanics, it could tunnel to lower energy states. That said, the barrier to entering the true vacuum may perhaps be so high that it has not yet been overcome anywhere in the universe, making the false vacuum configuration long lived and somewhat stable. [21]

The string vacuum constructions appear to be incredibly vast and this leads to a picture where basically any effective field theory which looks at least semi-classically consistent can arise in string theory. That said if any consistent looking effective field theory is actually consistent, one could invert the problem and instead of trying to construct string vacua using complicated geometries with extra dimensions, one could simply consider an effective field that looks consistent and matches the experimental observations. [22] However, most choices actually won't work as not all consistent looking effective field theories are actually consistent. In [22] C. Vafa argues that the consistent looking effective quantum field theories coupled to gravity, which are inconsistent with a quantum theory of gravity are even more vast and form the so called

"Swampland".

2.2 On the Cosmological Implications of the String Swampland

Based on the Swampland picture of string theory, in [1] P. Agrawal, G. Obied, P. J. Steinhardt and C. Vafa developed two Swampland criteria and studied their implications for an accelerating universe, showing a strong tension when considering models with a cosmological constant and imposing tight constraints on the possible quintessence models.

The first criterion imposes a bound on the the range transversed by scalar fields in field space since as we go further a large distance d, we basically reach another point in the landscape where a tower of light modes appears and invalidates the effective Lagrangian of the field (eq.2). The bound is such that $\Delta \sim \mathcal{O}(1)$ in reduced Planck units. [23]

$$\mathcal{L} = \sqrt{-g}\Big[\frac{1}{2}R - \frac{1}{2}g^{\mu\nu}\partial_\mu\phi^i\partial_\nu\phi^j G_{ij}(\phi) - V(\phi) + ...\Big] \tag{2}$$

The second criterion imposes a lower bound on $\frac{\nabla_\phi V}{V} > c \sim \mathcal{O}(1)$ in reduced Planck units in any consistent theory of gravity where $V > 0$. This bound is motivated by the observed difficulty to construct any reliable de Sitter Vacua (a stable vacuum energy with positive energy density) and by experience with string constructions of scalar potentials. [24] By solving the equation of motion based on the action of the form shown in eq.2, in the slow roll limit[8] one obtains that:

$$\frac{1}{3}\frac{\nabla_\phi V}{V} \approx (1 + w) \tag{3}$$

where w is the respective equation of state parameter of the field.

These two criteria combined impose tight constraints on the parameters that govern periods of cosmic acceleration. In particular they can be applied also to test the inflationary model which proposes a period of exponential expansion in the early universe in order to solve the horizon[9] and flatness[10] problem. [15] However, it is easier to verify the Swampland conjectures in a regime that is more testable, namely the present period of acceleration due to dark energy.

In this regard, the second Swampland criterion already excludes the possibility that the current acceleration is the result of a positive cosmological constant since, according to eq.3 for $w = -1$, $\frac{\nabla_\phi V}{V} = 0$ which violates the bound of criterion 2 for which $\frac{\nabla_\phi V}{V} > c$. The only possible solution is therefore given by quintessence models which if accurately tuned can satisfy both criteria. [18]

---

[8]The slow-roll approximation implies both $\frac{1}{2}\dot{\phi}^2 \lll V(\phi)$ and $\ddot{\phi} \lll 3H\dot{\phi}$. [25]
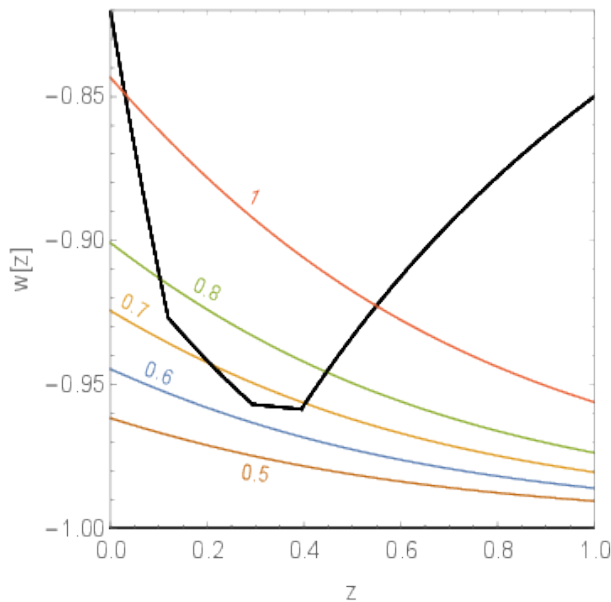
[9]The Horizon problem arises from the difficulty to explain the homogeneity of the universe at large scales with the fact that the initial universe consisted of at least $\sim 10^{83}$ regions which are causally disconnected, in other words regions that had not yet the time to communicate since light had still not been able to travel the distance within them. [15]

[10]As I explained earlier, the first angular peak of the power spectrum of the CMB provides the value of the curvature of the universe and, as confirmed by the last analysis of Planck 2018 is constrained to a very high confidence to $\Omega_k = 0$ which implies a perfectly flat universe. The flatness problem, at first exposed by Dicke and Peebles, refers to the extreme instability of such a result. [26]

To test the bounds imposed by the two Swampland criteria is sufficiently accurate to consider the special case of a canonically normalized field ϕ with an exponential potential of the form:

$$V(\phi) = V_0 e^{\lambda\phi} \tag{4}$$

for $\lambda = $ cost and with initial conditions given by the current constraints on $\Omega_\phi(z)$ and $w_\phi(z)$ from supernovae (SNeIa), cosmic microwave background (CMB) and baryon acoustic oscillation (BAO) measurements. [27]

Figure 4: The black curve shows the current observational 2σ bound on $w(z)$ for $0 < z < 1$ based on SNeIa, CMB and BAO data. [27] This is compared with the predicted $w_\phi(z)$ for exponential quintessence potentials with different values of constant λ under the constraint that $\Omega_\phi(z = 0) = 0.7$ and assuming $\Omega_\phi(z)$ becomes negligible at $z > 1$. From the plot, it is clear that the upper bound on $\lambda \sim 0.6$ (blue curve). Credit: [1]

Fig.4 compares the predictions of $w_\phi(z)$ for different values of λ with the current 2σ upper bounds on $w_\phi(z)$ for $0 < z < 1$. [27] This comparison shows that the upper bound on λ is 0.6 and therefore somewhat less than unity. [1] This constraint translates into a universal upper bound on c since the case for constant $\lambda(\phi) = c$ corresponds to the least constrained trajectory. A detailed proof of this statement goes beyond the scope of this paper, so for the interesting reader I suggest to refer to [1]. As shown in fig.4, for constant λ a trajectory is ruled out if c is bigger than 0.6. From here, it follows that every possible $\lambda(\phi)$ is ruled out if c is bigger than 0.6, leading to the universal bound $c \lessapprox 0.6$. [1]

The Swampland criteria also have implications for the possible futures of our universe given the current observational constraints on $\Omega_\phi(z)$ and $w_\phi(z)$ and the evolution of $\lambda(\phi)$. [1] In all the possible cases, it can be shown that the universe will undergo a phase transition within a few Hubble times at time $t_{\rm end} < [\frac{3\Delta}{2c\Omega_\phi}]H_0^{-1}$. [1] At this time $t_{\rm end}$, a new epoch for the universe will begin which may cause the production/appearance of a tower of light states and/or the transition from accelerated expansion to contraction.

3 Oxidised cosmic acceleration

The work of Steinhardt and Wesley as described in [2] [3] [28] received recent attention in the debate between the Landscape and Swampland pictures of string theory. Indeed by following a completely different approach, D. Wesley and P. Steinhardt developed a series of no-go theorems for constructing flat four-dimensional accelerating universes in theories with extra dimensions which have similar consequences with respect to the nature of dark energy and the fate of the universe. Specifically they also excluded the possibility of a universe dominated by a cosmological constant Λ, in favor of a quintessence model with time-varying w_{DE}.

Their conclusions were reached based on a set of assumptions that apply to a wide range of compactified models, including String theory. The key observation of these theorems is that the accelerated expansion of the large three spatial dimensions causes the compactified extra-dimensions to vary with time in such a way that it can become very difficult to keep them compact.

In this paper, I use the same approach of D. Wesley and P. Steinhardt to study different models of the universe given $w_{\text{DE}} = w_\phi$ as predicted in [1] for $\lambda = 0.5; 0.6; 07$.

In the following sections I will describe the main assumptions made and the general method used in this work; I will also introduce the main no-go theorems from the analysis done by D. Wesley and P.Steinhardt which will be useful for the purpose of this paper.

3.1 Methods and Assumptions

The no go theorems for accommodating cosmic acceleration in models with extra dimensions are based on a set of assumptions which are generally satisfied by many compactified theories with extra-dimensions and which will also constitute the base of my analysis.

1. The GR condition: both the higher dimensional theory and the 4d-theory are described by Einsten-Hilbert action up to small corrections which are regarded to be negligible.

2. The Flatness condition: the 4d-theory is spatially flat. This assumption is motivated by the cosmological observations. The current most updated constraints established the flatness of the spatial hypersurfaces at the 5×10^{-3} level with $\Omega_{\text{K}} = 0.0007 \pm 0.0019$ [8]

3. Boundedness condition: the extra-dimensions are bounded.

4. The metric condition: the metric of the higher dimensional theory is either Ricci-flat (RF) or Conformally Ricci-flat (CRF):

$$ds^2 = e^{2\Omega(t,y)}g_{\mu\nu}^{\text{FRW}}(t,x)dx^\mu dx^\nu + e^{-2\Omega(t,y)}h_{\alpha\beta}^{RF}(t,y)dy^\alpha dy^\beta \tag{5}$$

where $g_{\mu\nu}^{\text{FRW}}$ is the flat Friedmann-Robertson Walker metric taken to be:

$$g_{\mu\nu}^{\text{FRW}} = -\mathcal{N}(t)^2 dt^2 + \mathcal{A}(t)^2 \delta_{\text{mn}} dx^m dx^n; \tag{6}$$

Here, μ, ν are the indices along the 4 large dimensions with coordinates x^μ and α,β the indices along the k compact extra dimensions with coordinates y^α. Finally the extra dimensional metric $h_{\alpha\beta}$ is chosen to have finishing Ricci scalar with warp factor Ω either constant (RF) or time and spatial dependent (CRF).

5. The NEC condition: matter in both 4d and in the k extra dimensions satisfies the Null Energy condition (NEC) which states that:

$$T_{MN}n^M n^N \geq 0 \tag{7}$$

for any null vector n^M at a least one space-time point where T_{MN} is the stress energy tensor.

Condition n.3 mainly excludes volume-preserving transformations of a certain type and ensures that the curvature and warp term Ω have finite integrals over the compact direction which is needed to demonstrate some of the theorems. [3] Condition n.4 is motivated by common constructions in the literature. In particular for the no-go theorems that I will describe below we will use the CRF metric which occurs in many string theory models. [28] Finally condition n.5 is motivated by the fact that the NEC condition is not violated by any known matter field and usually its violation is a sign of a pathology in the theory. Indeed NEC violation is proven to lead to superluminal propagation, instabilities, problems with gravitational thermodynamics and exotic objects such as time machines and traversable wormholes. [3]

For a perfect fluid in four dimensions, the NEC requires $\rho + p \geq 0$. This can be extended also to the extra dimensions by defining $p_3 = \gamma_3^{\mu\nu}T_{\mu\nu}$, $p_{\mathrm{k}} = \gamma_{\mathrm{k}}^{\alpha\beta}T_{\alpha\beta}$ and ρ as the 0-0 component of the higher dimensional energy-momentum tensor T_{MN} where $\gamma_{3,\mathrm{k}}$ are respectively the 3×3 and $k \times k$ blocks of the higher dimensional space-time metric. In this scenario, for identifying cases where the NEC must be violated *Lemma 1* states:

Lemma 1 : if $\rho + p_3 < 0$ or $\rho + p_{\mathrm{k}} < 0$ for any space-time point then the NEC is violated.

Clearly if the average of $\rho + p$ over a certain region $\mathcal{M}$ is negative there will at least one space-time point inside $\mathcal{M}$ with $\rho + p < 0$ and thus the NEC is violated. This simple argument shows the importance of averaging over $\mathcal{M}$ as a useful tool to prove NEC violation and formulate no-go theorems for accommodating an accelerating universe. Specifically in [3] D. Wesley defines a specific one-parameter family of averages on $\mathcal{M}$. Given a function $Q(t,y)$ and a parameter A, $\langle Q \rangle_{\mathrm{A}}$ is defined as:

$$\langle Q \rangle_{\mathrm{A}} = \Big(\int Q e^{A\Omega} \sqrt{g} d^k y \Big) / \Big(\int e^{A\Omega} \sqrt{g} d^k y \Big); \tag{8}$$

In short, $\langle Q \rangle_{\mathrm{A}}$ is a weighted average of $Q(t,y)$ over the extra dimensions with weight factor $e^{A\Omega}$. Using the fact that the weight function in the A-average is positive definite, it follows another lemma for identifying cases where the NEC condition must be violated.

Lemma 2 : If $\langle \rho + p_3 \rangle_{\mathrm{A}} < 0$ or $\langle \rho + p_{\mathrm{k}} \rangle_{\mathrm{A}} < 0$ for any A and any space-time point then the NEC is violated.

3. OXIDISED COSMIC ACCELERATION

The no-go theorems arise from the solution of the Einstein's equations of motion of the higher dimensional theory after dimensional reduction. Following the convention used in [3], the time evolution of the higher-dimensional metric $h_{\alpha\beta}$ is expressed in terms of its trace component ξ and its traceless, shear component $\sigma_{\alpha\beta}$.

$$\frac{1}{2}\frac{dh_{\alpha\beta}}{dt} = \frac{1}{k}\xi h_{\alpha\beta} + \sigma_{\alpha\beta} \tag{9}$$

where both ξ and $\sigma_{\alpha\beta}$ are functions of t and y. The variable ξ basically determines the local expansion rate of the extra-dimensional space. Thus one can define the variable: ζ_{A} as

$$\zeta_{\mathrm{A}} = \frac{1}{H}\int e^{A\Omega}\xi\sqrt{h}d^k y \tag{10}$$

where H is the four-dimensional Hubble parameter and ζ_{A} represents the fractional growth of the extra-dimensional volume per Hubble time, using an A-dependent measure. [28] As explained in [28], for $A = 2$ eq.10 coincides with the volume measure that determines the four-dimensional Plank mass in warped compactifications and hence ζ relates to the variation of G by:

$$\frac{\dot{G}}{G} = -H\zeta \tag{11}$$

This relationship is very important because it states that if ζ is non zero then the volume of the extra dimensions changes with time causing also a change in the 4-dimensional gravitational constant G.

To obtain the Einstein's equations for the higher-dimensional theory, I express them, for convenience, in terms of the four-dimensional Einstein frame quantities using the following relation for the 4d effective scale factor a:

$$a(t) = e^{-\phi}\mathcal{A}(t) \tag{12}$$

where

$$e^{-\phi} = l^{-k}\int e^{2\Omega}\sqrt{g}d^k y \tag{13}$$

and l is the 4+k-dimensional Planck length. $e^{-\phi}$ can be thought as a measure of the volume of the compact space measured in 4+k-dimensional Planck lengths. Then, by solving the Einstein equations, one obtains:

$$e^{-\phi}\langle e^{2\Omega}(\rho + p_3)\rangle = (\rho_{4\mathrm{d}} + p_{4\mathrm{d}}) - \frac{k+2}{2k}\langle\xi\rangle_{\mathrm{A}}^2 - \frac{k+2}{2k}\langle(\xi - \langle\xi\rangle_{\mathrm{A}})^2\rangle_{\mathrm{A}} - \langle\sigma^2\rangle_{\mathrm{A}} \tag{14}$$

$$\begin{aligned}
e^{-\phi}\langle e^{2\Omega}(\rho + p_k)\rangle &= \frac{1}{2}(\rho_{4\mathrm{d}} + p_{4\mathrm{d}}) + 2\Big(\frac{A}{4} - 1\Big)\frac{k+2}{2k}\langle(\xi - \langle\xi\rangle_{\mathrm{A}})^2\rangle_{\mathrm{A}} \\
&\quad - \frac{k+2}{2k}\langle\xi\rangle_{\mathrm{A}}^2 - \langle\sigma^2\rangle_{\mathrm{A}} \\
&\quad + \Big[-5 + \frac{10}{k} + k + A\Big(-3 + \frac{6}{k}\Big)\Big]\langle e^{2\Omega}(\partial\Omega)^2\rangle_{\mathrm{A}} \\
&\quad + \frac{2+k}{2k}\frac{1}{a^3}\frac{d}{dt}(a^3\langle\xi\rangle_{\mathrm{A}})
\end{aligned} \tag{15}$$

12

The necessary calculations to obtain eq.13; 14; 15 go beyond the scope of this paper and are describe in detail in [3].

Based on Lemma.2, The NEC condition is violated if the right side of either eq.14 or 15 is less than zero.

The power of A-averaging comes into place now. In fact, by an accurate choice of A, one can make all the components that explicitly depend on A in both eq.14,15 non positive. Specifically, assuming $3 \leq k \leq 13$, this freedom is allowed for A in the following range:

$$\frac{10 - 5k + k^2}{3(k-2)} \leq A \leq 4 \tag{16}$$

For such choices of A eq.14; 15 can be rewritten in the simplified form:

$$e^{-\phi}\langle e^{2\Omega}(\rho + p_3)\rangle = \rho_{4\mathrm{d}}(1 + w) - \frac{k+2}{2k}\langle \xi \rangle_\mathrm{A}^2 + \text{non positive terms for } all \text{ A} \tag{17}$$

$$e^{-\phi}\langle e^{2\Omega}(\rho + p_k)\rangle = \frac{1}{2}\rho_{4\mathrm{d}}(1 + 3w) + \frac{2+k}{2k}\frac{1}{a^3}\frac{d}{dt}(a^3\langle \xi \rangle_\mathrm{A}) +$$
$$\text{non positive terms for } some \text{ A} \tag{18}$$

Where I used the fact that w is defined as the ratio between $\rho_{4\mathrm{d}}$ and $p_{4\mathrm{d}}$. In the discussion below, unless stated, I will always assume A to be in the allowed range of eq.16.

3.2 No-go Theorems for models that satisfy the NEC

As stated above, in order for a model to satisfy the NEC condition both eq.17 and 18 need to be non-negative. The first interesting case to analyze is that of the ΛCDM model where the dark energy is viewed as a cosmological constant with $w_\Lambda = -1$.

For $w = -1$, the first term of eq.17 is equal zero and the other two are non-positive. On the other hand, for $w = -1$ the first term of eq.18 is strictly negative and the last term is non-positive. Therefore to satisfy the NEC, both the second and third term of eq.17 need to be equal to 0 and the second and third of eq.18 to be respectively positive and 0. However, these two conditions cannot be satisfied simultaneously. Indeed, for the second term of eq.18 to be positive it requires ξ and/or its time derivative to be non-zero which is incompatible with keeping the middle term of eq.17 equal to zero. From here, it follows that w must be strictly greater than -1. It can be further shown that even for the case with $w > -1$ but close to -1, it is hard to always obey the NEC condition. In particular in [2], Wesley and Steinhardt show that there exists a $w_{\mathrm{transient}}$ between $-\frac{1}{3}$ and -1 such that w can remain in this interval only for a limited amount a time.

Indeed, for such $w < w_{\mathrm{transient}}$, to avoid the NEC violation in both eq.17 and 18 one needs both ξ close to zero and $\frac{d\xi}{dt}$ large, which is a condition that can only be maintained for a short period.

This analysis suggests the necessity of a dynamic form of dark energy with non constant w to ensure that the NEC condition is never violated. In fact, to reach $w < w_{\mathrm{transient}}$ in the first place,

w_{DE} has to be less than $w_{\text{transient}}$; then, in order to avoid NEC violation, w needs to become larger than $w_{\text{transient}}$ which is only possible if w_{DE} itself increases above $w_{\text{transient}}$. [2]

Another interesting case to analyze is given by $A = 2$. Indeed, for such choice of A, the change in the four-dimensional Newton's constant is directly related to ξ through eq.10 and 11. Therefore, the NEC inequalities given by eq.15 and 17 can be rewritten in terms of the fractional growth of the extra-dimensional volume per Hubble time ζ such that:

$$\zeta^2 \leq \frac{9(1 + w)}{2} \tag{19}$$

$$\frac{d\zeta}{dN} \geq \zeta^2 + \frac{3(w - 1)}{2}\zeta - \frac{9(1 + 3w)}{4} \tag{20}$$

Where $N = \ln(a)$ and a is the Einstein frame scale factor. To be more specific, k was chosen to be equal to 6 which corresponds to the number of extra-dimensions of String Theory. It is also important to notice that to obtain eq.20 and 19 both $\langle \sigma \rangle_A$ and $\langle e^{2\Omega}(\partial\Omega)^2 \rangle_A$ were set to zero. This choice was done to obtain a solution which allows the NEC condition to be satisfied for the largest period. [3] Indeed, given this choice of A, those terms are both non-positive and thus by setting them to zero, one allows the inequalities to be satisfied the longest. [29]

Eq.20 and 19 both strictly depend on w and as proven in detail in [28] to different ranges of w correspond different behaviours of ζ and consequently of the variation of G. The more interesting results from this analysis are listed below:
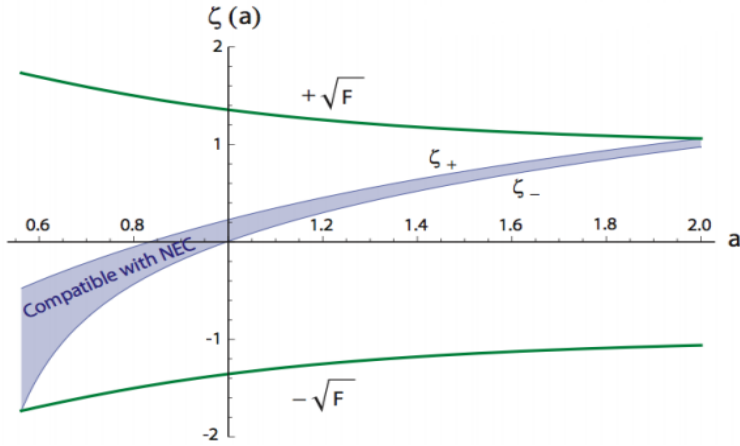
- A solution with constant Gravitational constant ($\zeta = 0$; $\frac{d\zeta}{da} = 0$) is only possible for $w \geq -\frac{1}{3}$

- A steadily accelerating solution ($\zeta = \text{cost}$; $\frac{d\zeta}{da} = 0$) is only possible for $w \geq w_{\text{trans}}$ where $w_{\text{trans}} = -5 + 2\sqrt{5}$.

- if $w < w_{\text{trans}}$ the right-hand side of eq.20 is positive definite $\forall \zeta$, so ζ must increase with time. Therefore, after a finite period, respectively the right side of eq.20 and the left side of eq.19 will become so large that they will violate the NEC condition encapsulated in these equations.

3.3 Constraints on time-variation of G for $w_{\text{DE}} = \text{cost} = -0.8$

The inequalities 20; .19 are the results of combining the higher-dimensional Einstein equations with the NEC condition. Since they are inequalities, they can be used to determine the range of possible $\zeta(a)$ trajectories and consequently the range of allowed variation of G that satisfy the energy condition. In particular from each ζ-curve one can obtain the value of the instantaneous variation of G ($\frac{\dot{G}}{G}\big|_{\text{today}}$) and of the secular variation of G ($\frac{G_{\text{BBN}}}{G}$) according to the following equations:

$$\frac{\dot{G}}{G}\bigg|_{\text{today}} = -H_0\Big[\zeta(1) \times 10^{-12}\Big]\text{yr}^{-1}$$
$$\frac{G_{\text{BBN}}}{G} = \int_{a_{\text{BBN}}}^{1} \frac{1}{a}\zeta(a)da \tag{21}$$

Where H_0 is taken to be 72. The first condition on ζ is given by eq.19 and it imposes that ζ must remain in the region between the two outer curves equal to $\pm\sqrt{F}$ where $F = \frac{9(1+w)}{2}$. To impose the constraints derived from the differential inequality eq.20, it suffices to consider ζ trajectories that saturate the inequality for different initial conditions (ICs) on ζ. [28] Wesley and Steinhardt considered the ζ trajectories bounded by $\zeta_{\pm}$. ζ_{-} is defined as the solution obtained by saturating eq.20 using the most negative initial value for ζ at the beginning of the accelerating epoch ($a_0 \approx 0.6$) allowed by 19. ζ_{+} is obtained in the same way, but uses the largest possible initial value for ζ such that it does not cross over $\sqrt{F}$ by a=2.

Figure 5: The constraints on ζ imposed by the NEC-inequalities 19 and 20 for a flat matter-quintessence model with $\Omega_{\mathrm{DE}}^0 = 0.74$ and $w_{\mathrm{DE}} = -0.8$. The upper and lower curves are the limits $\pm\sqrt{F}$ obtained from 19. All $\zeta(a)$ trajectories which are compatible with NEC must lie within the central band bounded by $\zeta_{\pm}$ computed as explained in this section. Credit: [28]

Their results are shown in fig.5 and suggest that the universe will undergo a transition phase within 2 Hubble times when the range of allowed ζ trajectories will cross the $\sqrt{F}$ curve, violating the NEC condition. The entire range of ζ trajectories is also essentially consistent with the experimental limits cited in [28] which I report below, at roughly 3σ.

$$\left.\frac{\dot{G}}{G}\right|_{\mathrm{today}} = (0 \pm 5) \times 10^{-12}\mathrm{yr}^{-1}$$
$$\frac{G_{\mathrm{BBN}}}{G} = 1^{+0.20}_{-0.16} \tag{22}$$

That said, it is important to emphasize the set of assumptions that were made in this analysis to explain how my approach will differ and results in a different strategy to find a set of allowed ζ trajectories:

1. It is assumed that for $w > -\frac{1}{3}$, ζ trajectories could be driven incredibly fast to zero, in such a way that the secular change in G was computed only during the period of cosmic acceleration.(for $a_0 \leq a \leq 1$)

2. w_{DE} is taken to be constant and equal to -0.8 with $\Omega_{\mathrm{DE}}^0 = 0.74$.

3.4 Constraints on time-variation of G for "stringy" $w_{\text{DE}} = w_\phi(a)$

In the analysis I performed, I dropped both assumptions 1 and 2. Indeed, there is no reason to assume that G can only change during the period of cosmic acceleration and as I will show in the next figures if not perfectly tuned the ζ trajectories tend to assume either very large or very small values as $a < a_0$[11]. Secondly, I will consider models with w_{DE} as predicted by the analysis in [1] for exponential quintessence potentials which respect the observational constraints on Ω_{DE}^0 and w_{DE}. As clearly shown in fig.4, the upper bound on $\lambda = 0.6$,however in this discussion I will initially also consider models with $\lambda = 0.5; 0.7$ to show how the ζ trajectories and the consequent costraints on the variation of G change according to λ.

In fig.9 I plotted the $\pm\sqrt{F}$ curves of the different time-changing w_{DE} for $\lambda = 0.5; 0.6; 0.7$ in comparison to the model of constant w_{DE} used by Wesley and Steinhardt in [28].

Generally, the $\pm\sqrt{F}$ curves shrink more firmly for $a > 1$ in the case of a time-changing w_{DE}. Specifically the smaller the value of λ the larger is the shrinking. The $\pm\sqrt{F}$ are uniquely determined by w which for the case of a matter-quintessence dominated universe is determined as explained in app.A.4. The resulting $w(a)$ curves for all the different models considered are plotted in fig.8.

Finally, in this analysis, I will also use the most updated value for the constraint on $\left.\frac{\dot{G}}{G}\right|_{\text{today}}$ from improvements in the ephemeris of Mars together with improved data and modeling of the effects of the asteroid belt. [30] The new constraint improves from the previous one used in [28] by roughly 2 orders of magnitude such that:

$$\left.\frac{\dot{G}}{G}\right|_{\text{today}}^{\text{NEW}} = (0.014 \pm 0.2) H_0 \times 10^{-14}\text{yr}^{-1} = (0.0947 \pm 1.35) \times 10^{-13}\text{yr}^{-1} \tag{23}$$

where in this analysis H_0 is taken to be 67.66 [8] according to the latest results published by the Planck mission.
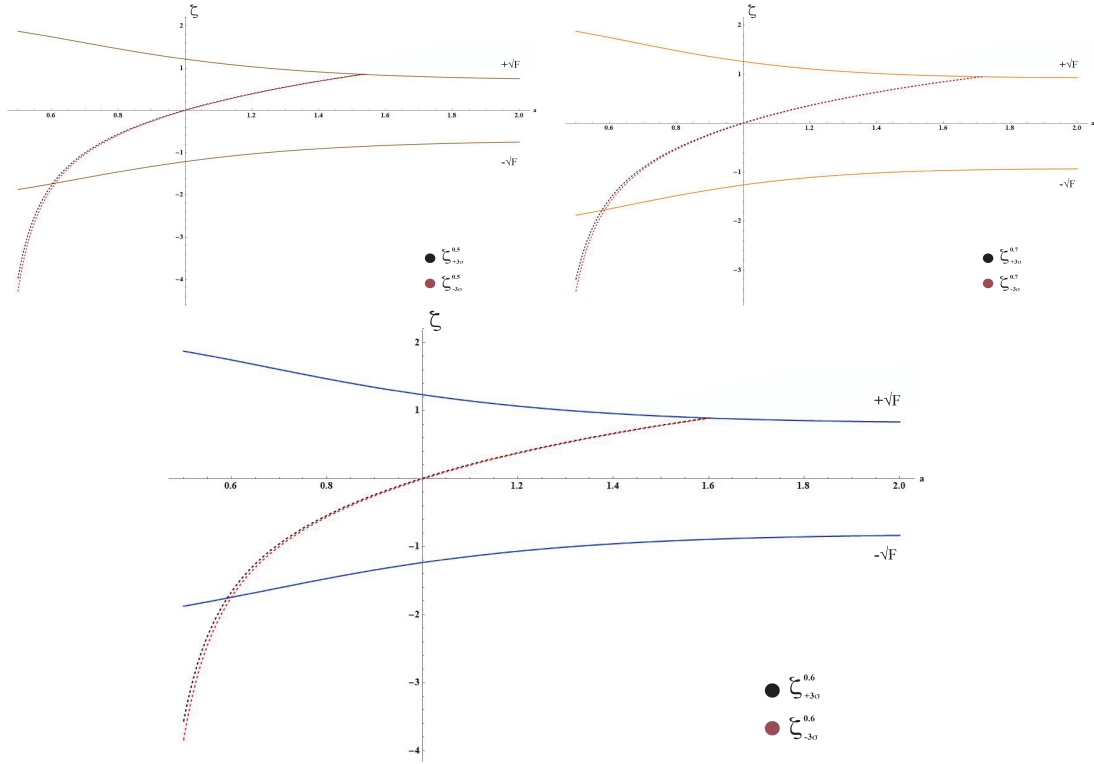
To explore all the ζ trajectories consistent with both constraints on the variation of G I will simply solve the saturated inequality 20 for different ICs for ζs, which can be arranged in two separated classes:

1. Define $\zeta_{\pm 3\sigma}$, given by imposing ICs at $a = 1$ such that

$$\zeta_{\pm 3\sigma}(1) = -(0.00014 \pm 3\sigma) \tag{24}$$

   where $\sigma = 0.002$ in order to obtain all the ζ trajectories bounded by the updated constraint on the instantaneous change in G at 3σ.

2. Define a set of ζ trajectories with ICs $\zeta(a_0) = 0$ for increasing values of a_0 from 0.09 up to 0.6, in the attempt to obtain all the ζ trajectories bounded by the constraint on the secular change in G at 3σ.
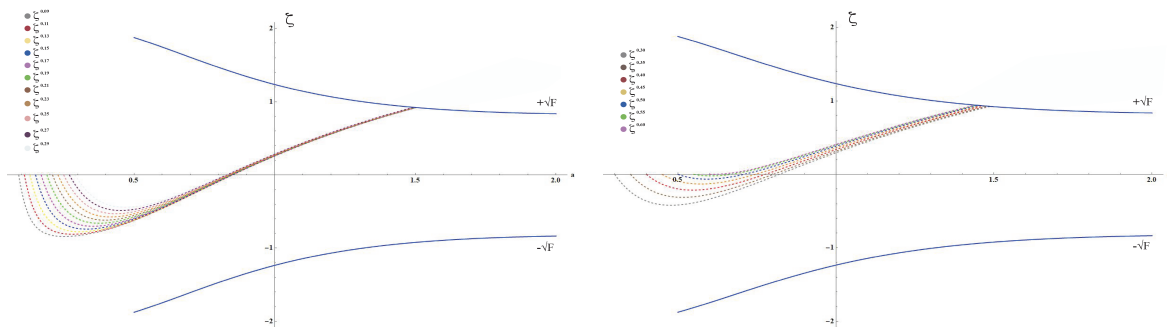
Figure 6: On Top it respectively refers to the case of $\lambda = 0.5$ (left) and $\lambda = 0.7$(right); at Meanwhile, the plot at the bottom represents the upper bound case for $\lambda = 0.6$. In each plot the dotted black and red curves represent the ζ trajectories given by the IC: $\zeta(1) = 0.00014 \pm 3\sigma$ where $\sigma = 0.002$ ($+3\sigma$ black curve; -3σ red curve). For all choices of λ, the $\zeta_{\pm 3\sigma}$ trajectories go to large negative values for $a < 0.6$, violating strongly the $\frac{G_{\mathrm{BBN}}}{G}$ constraint. Moreover, for all choices of λ the ζ trajectories violate the NEC condition for $a \approx 0.6$ entering the forbidden region below the $-\sqrt{F}$ curve.

ζ **trajectories for ICs:** $\zeta(1) = 0.00014 \pm 3\sigma$ **where** $\sigma = 0.002$ As shown in fig.6, all the $\zeta_{\pm 3\sigma}$ trajectories for every choice of λ assume large negative values for $a < 0.6$ drastically impacting the value of $\frac{G_{\mathrm{BBN}}}{G}$. In table.1 I reported the resulting values of $\frac{G_{\mathrm{BBN}}}{G}$ for all the possible $\zeta_{\pm 3\sigma}^{\lambda}$ computed according to eq.21 for $0.5 \leq a \leq 1$. I used as initial value for a 0.5 simply because even by only computing the integral in this range, the resulting $\frac{G_{\mathrm{BBN}}}{G}$ values already strongly violate the observational constraint for the secular change in G at 3σ.

Moreover in fig.6, one can also observe that all the ζ trajectories cross the $-\sqrt{F}$ curve at $a \approx 0.6$ entering the forbidden region by the energy condition. Therefore, all such models have to be ruled out since they both violate the observational constraint on the secular change in G and the NEC-condition for all $a < 0.6$.

ζ **trajectories for ICs:** $\zeta = 0$ **for** $0.09 \leq a \leq 0.6$ From this case, I will only analyze these ζ trajectories for the case of the best fitting w_{DE} with $\lambda = 0.6$. Indeed, as I will show shortly, for

---

[11]a_0 is defined as the value of the scale factor at which corresponds the beginning of the accelerating epoch

Figure 7: On Top it respectively refers to the case of $\lambda = 0.5$ (left) and $\lambda = 0.7$(right); at Meanwhile, the plot at the bottom represents the upper bound case for $\lambda = 0.6$. In each plot the dotted black and red curves represent the ζ trajectories given by the IC: $\zeta(1) = 0.00014 \pm 3\sigma$ where $\sigma = 0.002$ (+3σ black curve; -3σ red curve). For all choices of λ, the $\zeta_{\pm 3\sigma}$ trajectories go to large negative values for $a < 0.6$, violating strongly the $\frac{G_{\text{BBN}}}{G}$ constraint. Moreover, for all choices of λ the ζ trajectories violate the NEC condition for $a \approx 0.6$ entering the forbidden region below the $-\sqrt{F}$ curve.

this choice of ICs the ζ trajectories violate so strongly the constraint on $\frac{\dot{G}}{G}$ that changing λ by ± 0.1 would not make any significant difference.

Among these ζ trajectories, one can distinguish two sub-groups. For the ζ-curves with IC $\zeta = 0$ for $0.09 \leq a \leq 0.29$, All the ζ trajectories remain negative until the reach 0, drastically impacting the secular change in G. (refer to fig.7).In particular, $\frac{G_{\text{BBN}}}{G}$ is consistent with the observational constraint at roughly 3σ only for the ζ trajectories with a_0 in the range $0.17 \leq a_0 \leq 0.29$ and 2σ for $0.27 \leq a_0 \leq 0.29$. An interesting characteristic of this band of ζs is their behaviour for $a \geq 1$. Specifically all the ζ trajectories seem to converge reporting very similar values for $\frac{\dot{G}}{G}$ which all lie strongly outside the 3σ range of the updated observational constraint.

The second subgroup corresponds to all the ζ curves with IC $\zeta = 0$ for $0.3 \leq a_0 \leq 0.6$ (refer to fig.7). For $a \leq 0.6$, to increasing value of a_0 correspond ζ trajectories with smaller negative values until the limiting case $\zeta^{0.6}$[12]. This implies that for the ζ with larger a_0 correspond larger values of $\frac{G_{\text{BBN}}}{G}$ which is consistent to the observational constraint at 1σ level for all the considered ζ trajectories, expect for $\zeta^{0.3}$. However on the other hand, for larger a_0 ζ curves also assume larger values at $a = 1$, violating the updated $\frac{\dot{G}}{G}$ constraint well above the 3σ range and even more firmly than the first subgroup.

Overall all these NEC/CRF family of models have be ruled out since they don't satisfy the constraints on the variation of G at the 3σ level.

4   Conclusions

In this paper I have shown the difficulty of providing working examples of ζ trajectories that satisfy both the observational constraints on the variation of G and that do not violate

---

[12]ζ trajectory defined such that $\zeta(0.6) = 0$

the energy condition. These results were accomplished by assuming a flat matter-quintessence universe characterized by the equation of state parameter w_{DE} of a exponential quintessence potential which best fits the observational constraints on Ω^0_{DE} and w_{DE}.

All the NEC/CRF models that I constructed violated strongly one of the two constraints on the variation of G, in particular imposing ICs to keep $\left.\frac{\dot{G}}{G}\right|_{\mathrm{today}}$ fixed within the 3σ range caused the $\frac{G_{\mathrm{BBN}}}{G}$ to be completely off its observed value and viceversa. It would be interesting to show if this is a feature shared by all NEC/CRF models since in that case, we could possibly rule out entirely all this class of models.

If this was confirmed, in order to recover theories obtained by compactification from higher dimensions, one would have to investigate rather exotic solutions such as allowing the NEC to be violated or constructing models in which the higher-dimensional theory is not fully described by Einstein's theory of General Relativity for instance by introducing non negligible higher derivative terms.

A General Relativity, Friedman eqs and other useful relations

A.1 Foundations of GR

Einstein's theory of General Relativity (GR) has its foundations on the equivalence principle which states the equality between gravitational and inertial mass:

$$m_{\mathrm{g}} = m_{\mathrm{i}} \tag{25}$$

This principle is a remarkable fact since it implies that the property that determines the resistance to accelerating in response to the gravitational force, is equivalent to the property that determines the resistance to accelerating in response to any force. [31] In other words there is no way to distinguish between simple linear acceleration and gravitational acceleration caused by a massive body. [32]

The equivalence principle allows for a geometrical interpretation of the gravitational field where the spacetime is curved by the presence of mass.[13] The curvature of spacetime is therefore related to the energy components and their distribution. This relation is determined by the Einstein's field equations which can be derived by the Einstein-Hilbert action (eq.26) through the principle of least action. It is important to notice that in the discussion below and throughout the entirety of this paper I use reduced Planck units, $8\pi G = 1$.

$$S = \int R\sqrt{-g}d^4x \tag{26}$$

$$R_{\mu\nu} - \frac{1}{2}Rg_{\mu\nu} = T_{\mu\nu} \tag{27}$$

The left hand side of the equation measures the curvature of spacetime, meanwhile the right side gives us a measure of the energy and momentum contained in it. In particular, $R^{\mu\nu}$, the so called Ricci Tensor, is the trace of the Riemann curvature tensor, a four-component tensor which contains all the information about curvature and which is fully determined by the metric of spacetime $g^{\mu\nu}$. R is the Ricci scalar which is simply defined as the trace of the Ricci Tensor and provides a measure of the scalar curvature of spacetime. $T_{\mu\nu}$ is a symmetric two-index tensor called the energy-momentum tensor and, as can be inferred by its name, it contains all the necessary information about the energy and momentum of the matter fields, which act as a source for gravity. The components of $T_{\mu\nu}$ are determined by the flux of the μth component of momentum in the νth direction. [25] In the case of a perfect fluid, once that is isotropic and homogeneous, the energy momentum tensor takes the simplified form of eq.28 where u is the four-velocity vector of a fluid element, ρ the energy density and p the pressure.

$$T_{\mu\nu} = (\rho + p)u_\mu u_\nu - pg_{\mu\nu} \tag{28}$$

---

[13]to be more precise I should use the term mass-energy since in the theory of GR mass and energy are interchangeable as described by the well-known equation $E = mc^2$

A. GENERAL RELATIVITY, FRIEDMAN EQS AND OTHER USEFUL RELATIONS

A.2 The Friedman equations

Another important feature of the universe is the so called "Cosmological principle" which states that, on large scale, the universe is homogeneous and isotropic.

The Cosmological Principle was initially taken as an assumption and only by the end of the 20th century it was confirmed by measurements of the CMB and redshift surveys. [33] The homogeneity and isotropy of the universe is crucial because it allows us to reduce the Einstein's equations to 2 simple partial differential equations known as the Friedman equations. The Friedman equations are the dynamical equations of a homogeneous and isotropic universe and describe the evolution of the universe where the spatial curvature is taken as a function of time, allowing the possibility of a non stationary universe with positive or negative curvature, depending on the amount of matter and radiation contained in it. [34] The metric that describes such an homogeneous and isotropic universe is called the Robertson-Walker Metric and can be written in the form:

$$ds^2 = dt^2 - a^2(t)(\frac{1}{1 - kr^2}dr^2 + r^2d\theta^2 + r^2sin^2(\theta)d\phi^2) \tag{29}$$

The metric describes an homogeneous and isotropic universe respectively because of the spherical symmetry and because it does not have crossed terms between time and space which implies that there is not any privileged direction. [34] The time variable in the metric is the cosmological proper time defined as the time measured by an observer who sees the universe expanding uniformly around him. The spatial variables above (r, ϕ, θ) are called comoving coordinates and are defined to be constant with time if the expansion/contraction of the universe is homogeneous and isotropic. [31] The scale factor $a(t)$ is a dimensionless function that describes the growth or contraction of distances over time and finally the factor k is called the curvature constant and can take one of three values: $k = 1$ for a positive spatial curvature; $k = -1$ for a negative spatial curvature and $k = 0$ for a spatially flat universe.

the Friedman equations are the result of the combination of eq.27, 28 and 29 and in this paper they will represent the framework for studying the dynamics and evolution of the universe:

$$(\frac{\dot{a}}{a})^2 = \frac{\rho_{tot}}{3} - \frac{k}{a^2} \tag{30}$$

$$(\frac{\ddot{a}}{a}) = -\frac{1}{6}(\rho_{tot} + 3p_{tot}) \tag{31}$$

where respectively ρ_{tot} and $_{tot}$ correspond to the sum of the energy densities and pressures of the i elements that compose the universe. In this paper, I will consider models in which the universe contains three major components: matter (dark and byronic), radiation and dark energy.[14]

The Friedman equations can be rewritten in many forms and rearranged in several ways to emphasize different factors that impact the evolution of the universe. Below, I report the 3

---

[14]Please refer to sec.1 for a comprehensive introduction to the concept of dark energy.

equations which will be more useful for the purpose of this paper. For each of them I will define all their components but I will not attempt to derive them. For the interested reader, I suggest to refer to any introductory General Relativity manual such as [35].

$$\sum_i \Omega_{\mathrm{i}} + \Omega_{\mathrm{k}} = 1 \qquad \text{(F. Eq.1)} \tag{32}$$

$$H^2 = \frac{1}{3}\rho_{\mathrm{tot}}; \qquad \text{(F. Eq.2)} \tag{33}$$

$$\frac{\ddot{a}}{a} = -\frac{1}{6}\rho_{\mathrm{tot}}(1 + 3w); \qquad \text{(F. Eq.3)} \tag{34}$$

where:

$$\begin{aligned} \Omega_{\mathrm{i}} &= \frac{\rho_{\mathrm{i}}}{3H^2}; \qquad \Omega_{\mathrm{k}} = -\frac{k}{a^2 H^2}; \\ H &= \frac{\dot{a}}{a}; \qquad w = \frac{\rho_{\mathrm{tot}}}{p_{\mathrm{tot}}}; \end{aligned} \tag{35}$$

H is the well known Hubble parameter, at first introduced by Hubble to describe the relationship between distance and red-shifts of galaxies to provide evidence for an expanding universe.[15] The density parameters Ω_{i} provide a way to describe the fractional energy density of each of the i components of the universe. This general definition can be further extended to include the curvature term in such a way that eq.32 can be seen as a statement of energy conversation for the entire universe. If I increase Ω for any i component or for the curvature k, some other Ω has to decrease in order to keep the sum to unity.

It is important to notice that in both eq.33;34 I assumed the universe to be spatially flat with $\Omega_{\mathrm{k}} \approx 0$. This assumption is motivated by mounting evidence that has accumulated in the last 50 years. The most recent constraint was obtained by the Planck mission in 2018 and it measured $\Omega_{\mathrm{k}} = 0.0007 \pm 0.0019$. [8].

A.3 The equation of state parameter w and the evolution of ρ_i

In eq.34 I also introduced the equation of state parameter w whose value plays a crucial role in determining the dynamics of the universe over time. Indeed, for $w < -\frac{1}{3}$, $\frac{\ddot{a}}{a} > 0$ which implies the universe is accelerating. On the other hand if $w \geq \frac{1}{3}$ the universe is either decelerating or steadily-evolving.[16] The definition of w can be extended to each of the i elements of the universe such that $w_{\mathrm{i}} = \frac{p_{\mathrm{i}}}{\rho_{\mathrm{i}}}$. One can rewrite w in terms of w_i and Ω_i as follows:

$$w = \sum_i \Omega_i w_i \tag{36}$$

---

[15]the red-shift z refers to the stretching of the emitted wavelength of an electromagnetic radiation (such as light) and is defined as $z = \frac{\lambda_{\mathrm{obs}} - \lambda_{\mathrm{em}}}{\lambda_{\mathrm{obs}}}$ where λ_{em} and λ_{obs} are respectively the emitted and observed wavelength. In the picture of the expanding universe, the red-shift of electromagnetic waves is simply caused by their travelling through an expanding space which stretches out their wavelength.

[16]Expanding if $a > 0$ and contracting for $a < 0$.

Eq.36 emphasizes the fact that w and consequently the dynamics of the universe depends on the elements by which the universe is composed and their relative fraction. w_i also determines the evolution of each of elements of the universe over time. Indeed by combining the continuity equation of a fluid contained in a volume $V = V_0 a^3$ (eq.37) with the Friedman equations, one obtains a differential equation (eq.38) whose solution uniquely determines the evolution of ρ_i given its current value ρ_i^0 and $w_i(a)$. (eq.39) [31]

$$\frac{d(\rho_i V)}{dt} = -p_i \frac{dV}{dt} \qquad \text{(Continuity eq.)} \tag{37}$$

$$\frac{\dot{\rho}_i}{\rho_i} = -3H(1 + w_\mathrm{i}) \qquad \text{(Continuity eq. \& Friedman eq.)} \tag{38}$$

$$\rho_i(a) = \frac{1}{a^3} \rho_i^0 e^{\frac{3}{2} \int_0^a w(a) da^2} \tag{39}$$

For the case of matter and radiation, $w(a)$ is constant and is respectively equal to: [31]

$$w_\mathrm{m} = 0; \qquad w_\gamma = \frac{1}{3}; \tag{40}$$

Usually eq.39 is given in terms of the redshift z which is related to the scale factor a by the following relation: [31]

$$a = \frac{1}{(1 + z)} \tag{41}$$

A.4 Important relations for a universe matter and dark-energy dominated

In a universe dominated by matter and dark energy, $w = \Omega_\mathrm{DE} w_\mathrm{DE}$ since $w_\mathrm{m} = 0$ and w, the total equation of state parameter, is given by eq.36. Now, by combining the definition of density parameters Ω_i with eq.39, one obtains an equation for the ratio of Ω_m to Ω_DE such that:

$$\frac{\Omega_\mathrm{m}}{\Omega_\mathrm{DE}} = \frac{\rho_m}{\rho_\mathrm{DE}} = \frac{\Omega_\mathrm{m}^0}{\Omega_\mathrm{DE}^0} e^{-\frac{3}{2} \int_0^a w_\mathrm{DE}(a) da^2} \tag{42}$$
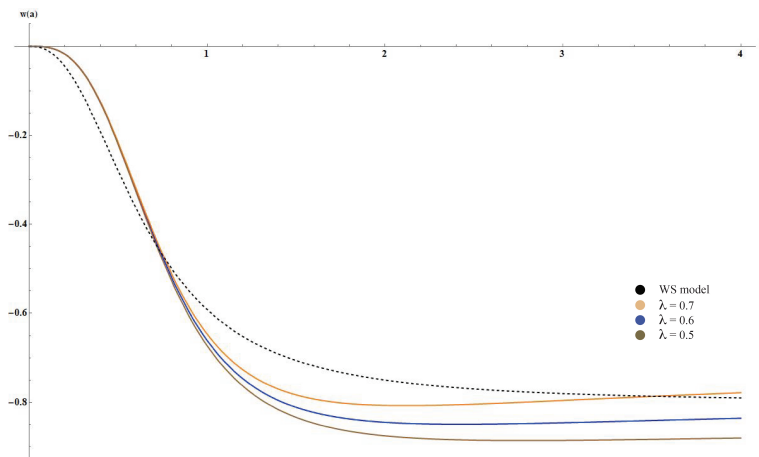
Finally, recalling that the sum of all the density parameters has to be unity, eq.42 can be rewritten as an equation for Ω_DE in terms of Ω_DE^0 and $w_\mathrm{DE}(a)$ of the following form:

$$\Omega_\mathrm{DE}(a) = \left[\left(\frac{1}{\Omega_\mathrm{DE}^0} - 1 \right) e^{-\frac{3}{2} \int_0^a w_\mathrm{DE}(a) da^2} \right]^{-1} \tag{43}$$
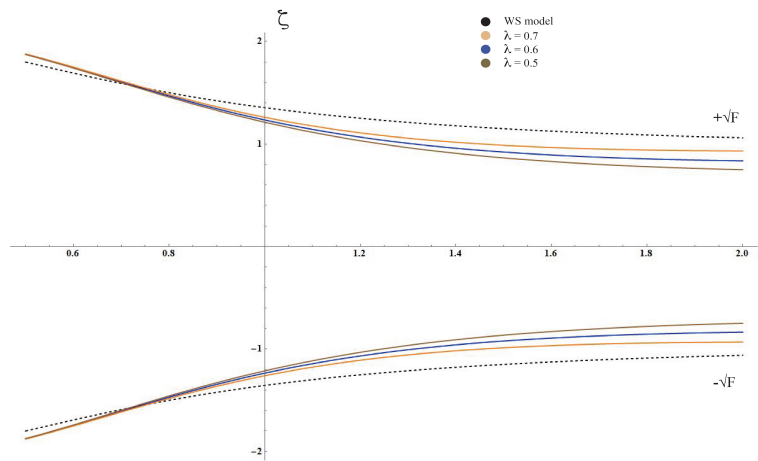
B   Relevant Plots and Tables

Constraints on the evolution of G for the different NEC/CRF models produced					
ζ trajectories with ICs $\zeta(1) = 0.00014 \pm 3\sigma$ where $\sigma = 0.002$					
ζ-curves:	$\left.\frac{\dot{G}}{G}\right|_{\text{today}}$	$\frac{G_{\text{BBN}}}{G}$	ζ-curves:	$\left.\frac{\dot{G}}{G}\right|_{\text{today}}$	$\frac{G_{\text{BBN}}}{G}$
$\zeta_{+3\sigma}^{0.5}$	3.96×10^{-13}	0.425	$\zeta_{-3\sigma}^{0.5}$	-4.15×10^{-13}	0.406
$\zeta_{+3\sigma}^{0.6}$	3.96×10^{-13}	0.45	$\zeta_{-3\sigma}^{0.6}$	-4.15×10^{-13}	0.431
$\zeta_{+3\sigma}^{0.7}$	3.96×10^{-13}	0.477	$\zeta_{-3\sigma}^{0.7}$	-4.15×10^{-13}	0.458
ζ trajectories with ICs: $\zeta = 0$ for $0.09 \le a \le 0.6$					
$\zeta^{0.09}$	-1.75×10^{-11}	0.266	$\zeta^{0.11}$	-1.76×10^{-11}	0.321
$\zeta^{0.13}$	-1.76×10^{-11}	0.374	$\zeta^{0.15}$	-1.77×10^{-11}	0.426
$\zeta^{0.17}$	-1.79×10^{-11}	0.478	$\zeta^{0.19}$	-1.81×10^{-11}	0.528
$\zeta^{0.21}$	-1.83×10^{-11}	0.577	$\zeta^{0.23}$	-1.86×10^{-11}	0.625
$\zeta^{0.25}$	-1.89×10^{-11}	0.671	$\zeta^{0.27}$	-1.93×10^{-11}	0.716
$\zeta^{0.29}$	-1.97×10^{-11}	0.758	$\zeta^{0.30}$	-1.99×10^{-11}	0.778
$\zeta^{0.35}$	-2.13×10^{-11}	0.872	$\zeta^{0.40}$	-2.28×10^{-11}	0.948
$\zeta^{0.45}$	-2.45×10^{-11}	1.006	$\zeta^{0.50}$	-2.59×10^{-11}	1.045
$\zeta^{0.55}$	-2.70×10^{-11}	1.067	$\zeta^{0.60}$	-2.75×10^{-11}	1.075

Table 1: In this table I report the values of $\left.\frac{\dot{G}}{G}\right|_{\text{today}}$ $\frac{G_{\text{BBN}}}{G}$ calculated according to eq.21. For ζ trajectories with ICs $\zeta(1) = 0.00014 \pm 3\sigma$ where $\sigma = 0.002$, I computed $\frac{G_{\text{BBN}}}{G}$ only integrating back to $a = 0.5$ since even just by integrating in this short interval, the values of $\frac{G_{\text{BBN}}}{G}$ lie outside the 3σ range. In regards to the ζ trajectories with ICs: $\zeta = 0$ for $0.09 \le a \le 0.6$, they all strongly fail the updated $\left.\frac{\dot{G}}{G}\right|_{\text{today}}$ given by eq.23.

Figure 8: This plot shows a comparison between w corresponding to the three different cases of λ and the WS-model. Specifically the yellow curve corresponds to $\lambda = 0.7$; the blue curve $\lambda = 0.6$ and the brown curve $\lambda = 0.5$. w is calculated by the product of Ω_{DE} times w_{DE} where Ω_{DE} for the three different cases of λ is calculated by eq.43 with $\Omega_{\text{DE}} \approx 0.7$ according to the latest results from the Planck mission. [8] The respective $w_{\text{DE}}(a)$ for each value of λ are computed by simply converting the functions $w_\phi(z)$ from fig.4 in terms of a according to eq.41.

Figure 9: This plot shows a comparison between the model used by Wesley (WS model) considering $w_{DE} =$ cost $= -0.8$ (black-dashed curves); and the new model using $w_{DE}(a)$ as derived in The String theory paper. The yellow, blue and brown curves represent respectively the $\lambda = 0.7; 0.6; 0.5$ case. Generally, in comparison to the WS model, the curves shrink more firmly for increasing values of a, specifically the smaller λ the more they shrink.

References

[1] P. Agrawal, G. Obied, P. J. Steinhardt, and C. Vafa, "On the Cosmological Implications of the String Swampland," *Phys. Lett.*, vol. B784, pp. 271–276, 2018.

[2] P. J. Steinhardt and D. Wesley, "Dark Energy, Inflation and Extra Dimensions," *Phys. Rev.*, vol. D79, p. 104026, 2009.

[3] D. H. Wesley, "Oxidised cosmic acceleration," *JCAP*, vol. 0901, p. 041, 2009.

[4] A. G. Riess, A. V. Filippenko, P. Challis, A. Clocchiatti, A. Diercks, P. M. Garnavich, R. L. Gilliland, C. J. Hogan, S. Jha, R. P. Kirshner, B. Leibundgut, M. M. Phillips, D. Reiss, B. P. Schmidt, R. A. Schommer, R. C. Smith, J. Spyromilio, C. Stubbs, N. B. Suntzeff, and J. Tonry, "Observational evidence from supernovae for an accelerating universe and a cosmological constant," *The Astronomical Journal*, vol. 116, no. 3, pp. 1009–1038, sep 1998. [Online]. Available: https://doi.org/10.1086%2F300499

[5] P. S. J., G. Aldering, G. Goldhaber, R. Knop, P. Nugent, P. G. Castro, S. Deustua, S. Fabbro, A. Goobar, D. Groom, I. Hook, A. Kim, M. Kim, J. C. Lee, N. Nunes, R. Pain, C. Pennypacker, R. Quimby, C. Lidman, and a. The Supernova Cosmology Project, "Measurements of ĂŽÂ© and ĂŽâ° from 42 high-redshift supernovae," *The Astrophysical Journal*, vol. 517, p. 565, 01 2009.

[6] W. Hillebrandt and J. C. Niemeyer, "Type Ia supernova explosion models," *Ann. Rev. Astron. Astrophys.*, vol. 38, pp. 191–230, 2000.

[7] V. C. Rubin, N. Thonnard, and W. K. Ford, Jr., "Extended rotation curves of high-luminosity spiral galaxies. IV - systematic dynamical properties, SA through SC," *Astrophysical Journal, Part 2 - Letters to the Editor*, vol. 225, pp. L107–L111, 1978.

[8] N. Aghanim *et al.*, "Planck 2018 results. VI. Cosmological parameters," 2018.

[9] "The cosmic microwave background," *Berkley University*.

[10] J. P. Ostriker and P. J. Steinhardt, "Cosmic concordance," 1995.

[11] A. A. Starobinsky, "Dynamics of phase transition in the new inflationary universe scenario and generation of perturbations," *Physics Letters B*, vol. 117, pp. 175–178, Nov. 1982.

[12] S. M. Carroll, W. H. Press, and E. L. Turner, "The cosmological constant," , vol. 30, pp. 499–542, 1992.

[13] A. G. Riess, W. H. Press, and R. P. Kirshner, "Using Type IA supernova light curve shapes to measure the Hubble constant," , vol. 438, pp. L17–L20, Jan. 1995.

[14] M. Bolte and C. J. Hogan, "Conflict over the age of the Universe," , vol. 376, pp. 399–402, Aug. 1995.

[15] A. H. Guth, "Inflationary universe: A possible solution to the horizon and flatness problems," *Phys. Rev. D*, vol. 23, pp. 347–356, Jan 1981. [Online]. Available: https://link.aps.org/doi/10.1103/PhysRevD.23.347

[16] A. D. Linde, "A new inflationary universe scenario: A possible solution of the horizon, flatness, homogeneity, isotropy and primordial monopole problems," *Physics Letters B*, vol. 108, pp. 389–393, Feb. 1982.

[17] P. J. Steinhardt, "A quintessential introduction to dark energy," *Philosophical Transactions: Mathematical, Physical and Engineering Sciences*, vol. 361, no. 1812, pp. 2497–2513, 2003. [Online]. Available: http://www.jstor.org/stable/3559230

[18] R. R. Caldwell, R. Dave, and P. J. Steinhardt, "Cosmological imprint of an energy component with general equation of state," *Phys. Rev. Lett.*, vol. 80, pp. 1582–1585, 1998.

[19] K. Wray, "An introduction to string theory." [Online]. Available: https://math.berkeley.edu/~kwray/papers/string_theory.pdf

[20] T. D. Brennan, F. Carta, and C. Vafa, "The String Landscape, the Swampland, and the Missing Corner," *PoS*, vol. TASI2017, p. 015, 2017.

[21] "False vacuum." [Online]. Available: https://en.wikipedia.org/wiki/False_vacuum

[22] C. Vafa, "The String landscape and the swampland," 2005.

[23] H. Ooguri and C. Vafa, "On the Geometry of the String Landscape and the Swampland," *Nucl. Phys.*, vol. B766, pp. 21–33, 2007.

[24] G. Obied, H. Ooguri, L. Spodyneiko, and C. Vafa, "De Sitter Space and the Swampland," 2018.

[25] S. Carroll, S. Carroll, and Addison-Wesley, *Spacetime and Geometry: An Introduction to General Relativity.* Addison Wesley, 2004. [Online]. Available: https://books.google.com/books?id=1SKFQgAACAAJ

[26] S. Hawking and W. Israel, *General Relativity: an Einstein Centenary Survey.* Cambridge University Press, 2010. [Online]. Available: https://books.google.com/books?id=1fmXZwEACAAJ

[27] D. M. Scolnic *et al.*, "The Complete Light-curve Sample of Spectroscopically Confirmed SNe Ia from Pan-STARRS1 and Cosmological Constraints from the Combined Pantheon Sample," *Astrophys. J.*, vol. 859, no. 2, p. 101, 2018.

[28] P. J. Steinhardt and D. Wesley, "Exploring extra dimensions through observational tests of dark energy and varying Newton's constant," 2010.

[29] D. H. Wesley, "New no-go theorems for cosmic acceleration with extra dimensions," 2008.

[30] C. Will, *Theory and Experiment in Gravitational Physics.* Cambridge University Press, 2018. [Online]. Available: https://books.google.com/books?id=gf1uDwAAQBAJ

[31] B. Ryden, *Introduction to Cosmology.* Cambridge University Press, 2017. [Online]. Available: https://books.google.com/books?id=07WSDQAAQBAJ

[32] J. Callahan, *The Geometry of Spacetime: An Introduction to Special and General Relativity*, ser. Undergraduate Texts in Mathematics. Springer New York, 2013. [Online]. Available: https://books.google.com/books?id=Jl7hBwAAQBAJ

[33] P. Steinhardt, V. Mukhanov, V. Mukhanov, C. U. Press, and M. Viatcheslav, *Physical Foundations of Cosmology.* Cambridge University Press, 2005. [Online]. Available: https://books.google.com/books?id=1TXO7GmwZFgC

[34] J. A. Romeu, "Derivation of friedman equations." [Online]. Available: http://www.astro.caltech.edu/~george/ay21/Ay21_Lec02.pdf

[35] B. Schutz, *A First Course in General Relativity.* Cambridge University Press, 2009. [Online]. Available: https://books.google.com/books?id=GgRRt7AbdwQC